Environment- and Sequence-Dependent Modulation of the Double-Stranded to Single-Stranded Conformational Transition of Gramicidin A in Membranes†

David Salom,‡ Enrique Pérez-Payá,‡ Jeanick Pascal,§ and Concepción Abad*,‡

Departament de Bioquímica i Biologia Molecular, Universitat de València, E-46100 Burjassot, Spain, and Multiple Peptide Systems, 3550 General Atomics Court, San Diego, California 92121

Received April 1, 1998; Revised Manuscript Received July 8, 1998

ABSTRACT: The role of the membrane lipid composition and the individual Trp residues in the conformational rearrangement of gramicidin A along the folding pathway to its channel conformation has been examined in phospholipid bilayers by means of previously described size-exclusion high-performance liquid chromatography HPLC-based strategy (Bañó et al. (1991) *Biochemistry 30*, 886). It has been demonstrated that the chemical composition of the membrane influences the transition rate of the peptide rearrangement from double-stranded dimers to β-helical monomers. The chemical modification of Trp residues, or its substitution by the more hydrophobic residues phenylalanine or naphthylalanine, stabilized the double-stranded dimer conformation in model membranes. This effect was more notable as the number of Trp-substituted residues increased (tetra > tri > di > mono), and it was also influenced by the specific position of the substituted amino acid residue in the sequence, in the order Trp-9 ≈ Trp-13 > Trp-11 > Trp-15. Moreover, it was verified that nearly a full contingent of indoles (Trp-13, -11, and -9) is necessary to induce a quantitative conversion from double-stranded dimers to single-stranded monomers, although Trp-9 and Trp-13 seemed to be key residues for the stabilization of the β-helical monomeric conformation of gramicidin A. The conformation adopted for monomeric Trp → Phe substitution analogues in lipid vesicles resulted in CD spectra similar to the typical single-stranded $\beta^{6.3}$-helical conformation of gramicidin A. However, the Trp → Phe substitution analogues showed decreased antibiotic activity as the number of Trp decreased.

A current question in structure−function relationships for membrane and soluble proteins how does the primary sequence affect the protein structure and what is the influence of the local and global environments on the protein folding process. For integral membrane proteins it is generally recognized that both the membrane's hydrophobic core and the membrane/water interface constitute critical organizing elements (*1*, *2*). Examples of environment-dependent conformations have been reported for simple synthetic model peptides (*3*−*5*) and for gramicidin A, a naturally occurring antibiotic peptide (for recent reviews see refs *6* and *7*). In particular, recent studies with linear gramicidins have described how the interplay between the peptide sequence and the environment might ultimately dictate the final folded state of a membrane peptide (*8*, *9*).

Gramicidin A (gA) is a linear hydrophobic peptide with an L,D-alternating sequence: formyl-L-Val[1]-Gly[2]-L-Ala[3]-D-Leu[4]-L-Ala[5]-D-Val[6]-L-Val[7]-D-Val[8]-L-Trp[9]-D-Leu[10]-L-Trp[11]-D-Leu[12]-L-Trp[13]-D-Leu[14]-L-Trp[15]-ethanolamine. In the natural mixture of gramicidin, produced by *Bacillus brevis*, gramicidin B (5%) and C (15%) also exist, with phenylalanine and tyrosine residues in position 11, respectively. Because of its lack of charges, gA is water-insoluble, but it is soluble in organic solvents and it incorporates easily in lipid bilayers. The molecular structure and dynamics of gA are strongly environment-sensitive. In organic solvents the peptide exists in a conformational equilibrium between different monomeric and dimeric (intertwined double-stranded; ds) species (*10*−*15*). The conformational equilibrium is displaced toward double-helical conformations in nonpolar solvents as tetrahydrofuran (THF)[1] or dioxane, while in polar solvents, such as trifluoethanol (TFE), the monomeric species predominate (*11*, *13*, *15*−*18*). The lipid-induced folding of gA plays a determinant role in its biological function that resides in its ability to form dimeric single-stranded transmembrane channels, permeable to monovalent cations. Thus, for understanding the conformational dynamics of gA when incorporated into membrane bilayers, care must be taken in the incorporation methods used since the conformation of gA in bilayers shows a solvent history dependence (*19*−*26*), and the proportion between monomers and ds-dimers present in fresh gA-containing vesicles depends on those existing before

† This work was supported by Grants PB93-0359 and SAF97-0067 from DGICYT (Spain). D.S. was a recipient of a long-term postgraduate fellowship from the Generalitat Valenciana (Spain).

* To whom correspondence should be addressed.

‡ Universitat de València.

§ Multiple Peptide Systems.

[1] Abbreviations: DHPC, dihexadecyl-phosphatidylcholine; DMoPC, dimyristoleoyl-L-α-phosphatidylcholine; DMSO, dimethyl sulfoxide; DOPC, dioleoyl-L-α-phosphatidylcholine; DOPE, dioleoyl-L-α-phosphatidylethanolamine; DOPG, dioleoyl-L-α-phosphatidylglycerol; DOPS, dioleoyl-L-α-phosphatidylserine; DPoPC, dipalmitoleoyl-L-α-phosphatidylcholine; DPPC, dipalmitoyl-L-α-phosphatidylcholine; ds, double stranded; EPC, egg yolk phosphatidylcholine; POPC, 1-palmitoyl, 2-oleoyl-phosphatidylcholine; SDS, sodium dodecyl sulfate; SUV, small unilamellar vesicles; TFE, trifluoroethanol; THF, tetrahydrofuran.

S0006-2960(98)00733-8 CCC: $15.00
Published on Web 09/18/1998

in the organic solvent (*21*, *23*, *24*). In fact, when polar solvents are used to prepare the gA-containing bilayers the peptide adopts the single-stranded β-helical conformation (channel state), while when incorporated from nonpolar solvents, the ds-dimeric conformation predominates (non-channel structure) (*19*−*24*). However, in the lipid milieu the ds-dimeric conformation is a metastable state that slowly dissociates in a temperature-dependent process and that refolds into the channel conformation (*19*−*27*). The presence of a nonminimum energy conformational state, the ds-dimeric conformation, suggests that the folding path and hence the folding environment are critical for achieving a functional state. Thus, as an example, recent spectroscopic results indicated that a minimum lipid acyl chain length is necessary to stabilize the channel configuration (*26*) and that in lipids containing unsaturated fatty acids gA forms the double-helical conformation (*28*, *29*).

The gA transmembrane channels are formed by the transient N-terminal-to-N-terminal association of two single-stranded helical monomers in the β-conformation (*30*). Due to the alternating chirality, in the β-conformation the amino acid side chains are oriented toward the exterior of the helix, and interact with the lipid bilayer's hydrophobic core and the membrane/water interface. The channel state has each of the carboxy-terminal Trp residues oriented toward the hydrophilic bilayer surface, where the indole NH groups might hydrogen bond to polar groups of the phospholipids or directly to water molecules in the interface (*31*−*37*). Although extensive studies concerning the structure and properties of the gramicidin A channel have been addressed, our understanding of the molecular rationale that relies on the gramicidin channel formation is still incipient (*8*, *9*, *15*, *17*). The left-handed antiparallel double helix that predominates in low dielectric isotropic organic solvent (*17*, *38*) is converted to the right-handed single-stranded helix of the channel state in hydrated lipid bilayers (*27*). The driving force for this conformational rearrangement could emerge from the arrangement of the Trp within the lipid environment (*17*, *22*, *27*). The antiparallel ds-dimer might direct the indole nitrogens toward the bilayer surface when the structure untwists to form the amino-terminus-to-amino-terminus functional dimer. Recent HPLC (*8*) and NMR (*9*) studies showed that the replacement of the four Trp in gA by phenylalanines (gramicidin M) reverses the peptide conformational equilibrium in model membranes, that is, it dramatically favors the ds-dimeric peptide conformation. Thus, without the four indoles (i.e., gramicidin M) the antiparallel double-helical conformation of gramicidin is the minimum-energy conformational state in the bilayer (*9*). This structure, however, does not conduct ions (*29*, *39*). Therefore, indoles could be described as molecular triggers for the conformational interconversion of gA from double-stranded helices to single-stranded helices (channel state) in a lipid environment.

In the present study, by means of the previously described size-exclusion high-performance liquid chromatography HPLC-based strategy (*21*, *23*), the role of both the lipid environment and the individual Trp residues in the conformational rearrangement of gramicidin A has been examined. A detailed study of the parameters that control the ds-dimer/monomer interconversion would provide insights on the molecular determinants that drive the peptide in the membrane along the folding pathway to achieve the functional channel state. Peptide analogues with all four Trp residues chemically modified or replaced by less polar residues (phenylalanine or naphthylalanine) lacking H-bonding ability were studied. A series of 14 gramicidin analogues with systematic replacements of one, two, and three Trp residues by phenylalanine was synthesized by solid-phase multiple-peptide synthesis (*40*). In light of our present results, it seems that the chemical composition of the membrane has a small influence on the conformational preference of the peptide, although it influenced the transition rate from double-stranded to single-stranded helices in the membrane. Hence, we could conclude that the thermodynamically stable conformation of gA in membranes is the monomeric single-stranded structure. Furthermore, it has been demonstrated in the present paper that each Trp residue in gA has a specific contribution in the unwinding of double-stranded dimeric structures in the lipid bilayer, and in the stabilization of the monomeric (channel) configuration. To gain insight into the microenvironment of each single Trp residue in both double-stranded dimeric and monomeric structures, and into the backbone conformation of Trp → Phe substituted monomeric gramicidins, the chromatographic information has been complemented with data obtained from steady-state fluorescence and circular dichroism spectroscopies. The results are discussed in light of the current knowledge on the conformational behavior of gramicidin in model membrane systems.

MATERIALS AND METHODS

Materials. Gramicidin (a natural mixture predominantly composed of gramicidin A, ca. 85%) was purchased from Sigma Chemical Co. (St. Louis, MO) and was used without further purification. The analogue *N*-formyl gramicidin A was a generous gift from Dr. J. A. Killian (Centre for Biomembranes and Lipid Enzymology, University of Utrecht), and the analogue with four replacements of Trp by naphthylalanine (Nap), named gramicidin N (gN), was a gift of Dr. F. Heitz (CRBM, CNRS-INSERM, Montpellier, France). Boc- and Fmoc-protected amino acids, and Wang resin, were from Novabiochem (Switzerland). Egg yolk phosphatidylcholine (EPC) was purchased from Merck (Darmstadt, Germany) and purified according to the chromatographic method of Singleton et al. (41). Dihexadecyl-L-α-phosphatidylcholine (DHPC) was from Bachem (Bubendorf, Switzerland), whereas dimyristoleoyl-L-α-phosphatidylcholine (DMoPC) and dipalmitoleoyl-L-α-phosphatidylcholine (DPoPC) were from Avanti Polar Lipids Inc. (Alabaster, AL). All other phospholipids, sterols, and trehalose were from Sigma Chemical Co. THF and all other organic solvents were from Merck, either HPLC or spectroscopic grade.

Peptide Synthesis. The first 5 residues (from carboxy terminus) were coupled to the Wang resin with a 6-fold molar excess of Boc-amino acid and coupling reagents (hydroxybenzotriazole, diisopropylcarbodiimide). The remaining 10 residues were assembled using double couplings (2 h and overnight cycles) with 4-fold molar excesses of Fmoc-amino acid and coupling reagents. Cleavage of the peptidyl resins was effected by treatment with ethanolamine/dimethylformamide (50:50) for 12 h at 50 °C. Some of the peptides precipitated after cleavage from the resin; in those cases dimethylformamide was added to redissolve the peptide

before filtering off the resin. The filtered peptides were precipitated by the addition of 4 volumes of H_2O, dried, resuspended in methanol, dried with a N_2 stream, dissolved in acetic acid, and lyophilized. Details for the purification and characterization of these Trp substitution gramicidins have been previously reported (*42*). The synthetic gramicidins were named as follows: the native sequence (gA), four analogues with one Trp → Phe substitution (W9FgA, W11FgA, W13FgA, and W15FgA); six with two substitutions (W(9,11)FgA, W(9,13)FgA, W(9,15)FgA, W(11,13)FgA, W(11,15)FgA, and W(13,15)FgA), four with three substitutions (W(9,11,13)FgA, W(9,11,15)FgA, W(9,13,15)FgA, and W(11,13,15)FgA), and one with four substitutions (W(9,11,13,15)FgA, also named gM). These Trp substitution gramicidin analogues have been named with the abbreviation name of the native peptide, gA, preceded by the following: first, the one-letter code of the original amino acid; second, its sequence position(s); and third, the one-letter code of the substituting amino acid.

Preparation of Peptide-Containing Liposomes. Small unilamellar vesicles (SUV) containing gA (or any gramicidin analogue) were prepared by cosolubilization of lipid and peptide in a given organic solvent (TFE, to obtain mainly monomeric species, and THF to get predominantly ds-dimers). The solvent was rapidly evaporated under a nitrogen stream and later under high vacuum overnight to ensure complete removal of solvent. An aqueous solution (water, buffer, or trehalose solution) was then added, and the lipid was hydrated under vortexing for 5 min. The opaque suspension was sonicated for 15 min (5 min in the experiment with diunsaturated phospholipids) with a microtip probe (Vibra cell, Sonics and Materials, Inc., Daubury, CT) at power setting 4 and 50% duty cycle. Next, the samples were centrifuged for 15 min at 15000*g* to remove probe particles and the remaining multilamellar aggregates. All steps of the sample preparation were performed at 0 °C to minimize any conformational change of the peptides. All experiments were carried out above the phase-transition temperature of the lipids used.

Typically, the final concentration of phospholipid was 2 mM and the peptide 40 μM. The lipid content of the samples was chromatographically determined after evaporation of an aliquot in SpeedVac and redisolution in organic solvent. The phospholipid concentration was determined by normal-phase HPLC, as described by Mingarro et al. (*43*), whereas the sterol concentration was determined by reversed-phase HPLC, as described by New (*44*). The peptide concentration was determined using as molar absorption coefficients 13700 cm^{-1} M^{-1} for N-formyl gramicidin, 20600 cm^{-1} M^{-1} for gA′, and 22600 cm^{-1} M^{-1} for gA (*45*). For the analogues with Trp → Phe replacements, 5650 cm^{-1} M^{-1} for each Trp residue was considered. gN and gM were determined gravimetrically. The integrity of SUV preparations was controlled by negative-stain electron microscopy.

Size-Exclusion HPLC Procedure. Peptide conformers (monomers and ds-dimers) of gA and the different analogues were separated and quantified by analytical HPLC through a size-exclusion mechanism as previouly reported (*8, 14, 21*), using a Waters (Milford, MA) Ultrastyragel 1000 Å column eluted with pure THF. Briefly, when a few microliters of an aqueous gA-containing model membrane are injected directly onto the column, the phospholipid assemblies are immediately disrupted by the organic mobile phase, releasing the polypeptide conformational species to the eluent stream. Under these conditions, double-stranded helical dimers, which are stabilized by 28 intermolecular H-bonds, will remain intact upon vesicle disruption and elute as dimers. On the other hand, the single-stranded species (monomers and dimeric channels) elute as free monomers. The percentage of double-stranded dimers and β-helical monomers eluted from the column does not differ from the values originally present in the vesicles on the basis of the extremely slow ds-dimer/monomer transition undergone by gramicidin in THF (*14*). The flow rate was 1.0 mL/min, and the eluting peptides were detected at 280 nm, except for the analogue with four Trp → Phe substitutions, which was detected at 260 nm. All chromatographic measurements were made in triplicate, and the standard deviation was always <3%.

Circular Dichroism. CD measurements were performed with a Jovin-Yvon CD6 spectropolarimeter, using a 0.5-mm optical path length cell. Blank runs of vesicles in water were subtracted from the measured spectra of gramicidin-reconstituted samples. Ellipticity [θ] values were expresed on a mean residue basis, in units of deg cm^2 $dmol^{-1}$. Each reported spectrum was the average of three independent scans.

Fluorescence Measurements. Fluorescence excitation and emission spectra (uncorrected) were recorded on a Perkin-Elmer LS 50 spectrofluorometer, using 1-cm quartz cells. Excitation and emission slits with a nominal band-pass of 2.5 nm were used. In the emission spectra, the excitation wavelength was 280 nm, whereas in the excitation spectra, the emission wavelength was set to the emission maximum. All spectra of peptide-containing vesicles were corrected by subtracting blank runs corresponding to a sample of vesicles without peptide.

Antibiotic Assay. The antibiotic activity of each gramicidin analogue was determined against *Enterococcus faecium* (ATCC 10541) adapting the turbidimetric method described in FDA Title 21 Part 430.106. Each single assay was prepared using 5 mL of culture medium, 52 μL of a peptide solution at the appropiate concentration in DMSO, and 200 μL of a fresh bacterial culture (incubated 16−18 h at 37 °C). The samples were vortexed and incubated for 3.5 h at 37 °C. The optical density at 660 nm (OD_{660}) was used as a measurement of the bacterial growth. The concentration of peptide necessary to inhibit 50% of the bacterial growth (IC_{50}) was then determined for each peptide using a sigmoidal curve-fitting method.

Kinetic Models. Size-exclusion HPLC with apolar eluents permits the separation and quantification of single-stranded (including free monomers and N-terminus-to-N-terminus dimers), denoted as M, and double-stranded (M_2) species of linear gramicidins inserted in phospholipid vesicles, and the determination of the state of the following equilibrium at any given time:

$$M_2 \underset{k_{-1}}{\overset{k_1}{\rightleftharpoons}} 2M \qquad (1)$$

where k_1 and k_{-1} denote the forward and reverse rate constants, respectively. The accuracy of the HPLC measurements made feasible the chromatografic data fitting to this dimer/monomer equilibrium. The integrated rate describing

the approach to equilibrium is easily obtained by standard integration methods. The equation describing the change in ds-dimer concentration versus time is:

$$\ln\left(\frac{[M_2]_T^2}{[M_2]_e} - [M_2]\right) = \ln\left(\frac{[M_2]_T^2}{[M_2]_e} - [M_2]_0\right) + \frac{[M_2]_T + [M_2]_e}{[M_2]_T - [M_2]_e} k_1 t \quad (2)$$

where $[M_2]_0$, $[M_2]_e$, and $[M_2]$ refer to the ds-dimer's concentration at 0 time (freshly prepared samples), at equilibrium, and at any given time, t, respectively. $[M_2]_T$, being the total peptide concentration, referred to ds-dimers, which is different from $[M_2]_0$ because it is not experimentally possible to obtain fresh samples with 100% of ds-dimers.

An equivalent expression that describes the monomer concentration changes was also obtained:

$$\ln\left(\frac{[M]_T^2 - ([M]_T - [M])([M]_T - [M]_e)}{[M] - [M]_e}\right) = \ln\left(\frac{[M]_T^2 - ([M]_T - [M]_0)([M]_T - [M]_e)}{[M]_0 - [M]_e}\right) + \frac{[M]_e(2[M]_T - [M]_e)}{[M]_T - [M]_e} k_{-1} t \quad (3)$$

where $[M]_0$, $[M]_e$, and $[M]$ refer to the monomer concentration at 0 time, at equilibrium, and at any given time, t, respectively. $[M]_T$ represents the total peptide concentration referred to monomers.

All kinetic data (see below) were satisfactorily described by these equations, demonstrating that the changes observed are only due to the simple dimer/monomer equilibrium (eq 1). The kinetic constants were calculated by fitting the experimental data to one of these equations (eq 2 or 3).

RESULTS

Size-exclusion HPLC, in combination with CD, has proved to be a valuable technique to monitor conformational transitions of gramicidin A reconstituted in phospholipid model membranes (*14*, *21*, *23*). By making possible the physical separation and quantitation of membrane-inserted double-stranded dimers and β-helical monomers, it was demonstrated in previous studies that (i) a mixture of basically these two conformers in different proportions contributes to the observed "nonchannel" CD patterns, and (ii) the transition undergone by gramicidin from the nonchannel toward the channel configuration can be correlated with a quantitative conversion from double-stranded dimers to β-helical monomers (*23*, *24*). Taking advantage of this HPLC strategy we now report the results of a quantitative study directed to assess the role that both the lipid environment and the peptide Trp residues play in the conformational rearrangement of gramicidin A along the folding pathway to achieve the channel conformation.

(I) Lipid Environment Modulation of the Conformational Rearrangement of Gramicidin A. Lipid Headgroup Composition and Headgroup Hydration. The intertwined double-stranded dimeric conformation of gramicidin A is incorporated into the lipid bilayer when model membranes containing the peptide are prepared from nonpolar organic solvents (*9*, *17*, *21*, *23*, *27*). This state is a metastable structure that is kinetically trapped just above the phase-transition temperature of the lipid (*27*). Upon raising the temperature the ds-dimer undergoes a conformational transition toward the channel state (*23*, *27*) that can be described as the minimum-energy conformation in a bilayer environment. The conformational transition might be driven by the formation of hydrogen bonds between the four Trp residue side chains and the lipid polar heads and/or with interfacial water at the bilayer surface (*8*, *9*, *17*, *22*, *27*). Initially, we designed experiments in order to assess the potential contribution of these two kinds of hydrogen bonds in the unwinding of the double-stranded dimeric conformation of gA when incorporated into phospholipid bilayers. Thus, gA containing vesicles of DPPC (ester linkage) and DHPC (ether linkage) was prepared by cosolubilization of the peptide and lipid in THF, to achieve samples containing mainly ds-conformers (*21*, *23*). The time-dependent conformational transition from ds-dimers to β-helical monomers was monitored by HPLC (Figure 1). The mass fraction of ds-dimers and monomers can be directly determined at any given time from the chromatograms, as previously reported (*14*). The experiment was carried out at 50 °C (above the phase-transition temperature of the lipids) using unsonicated vesicles to avoid temperature-induced monomerization of the peptide during the sonication step (*23*). The monomerization rate and the equilibrium mass fraction of ds-dimers were similar in both DPPC and DHPC lipid bilayers (Figure 1). By fitting of the kinetic data to eq 2 (Materials and Methods), it was verified that the transition observed corresponded to a simple process of dissociation of ds-dimers (M_2) into monomers (M). Therefore, since the vesicles formed by either of these two lipids have nearly identical physical properties (*46*), it seems that an interaction of gA with the carbonyl group in the ester linkage is not necessary for the monomerization process.

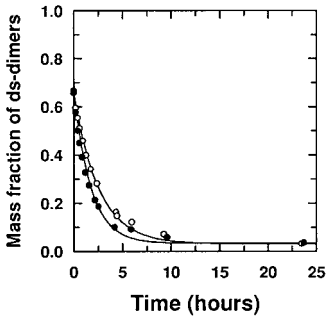

FIGURE 1: Variation of the mass fraction of gA in ds-dimers, as determined by HPLC, in unsonicated vesicles of DPPC (○) and DHPC (●) as a function of incubation time at 50 °C. The lines correspond to the fitting of the data to eq 2 (see the Materials and Methods section). The peptide concentration was 40 μM, and the peptide/lipid mole ratio was 1:50. It was also corroborated that, in sonicated vesicles containing gA monomers as the starting structure (cosolubilized from TFE), the equilibrium mass fraction of the ds-dimers was less than 0.03 in these two bilayers.

The role of the hydration water of the lipid interface polar headgroups was investigated by HPLC using EPC SUV suspensions containing in the bulk aqueous phase increasing concentrations of trehalose, a sugar with a dehydratant effect on the bilayer (*47*, *48*). At the equilibrium, the most stable

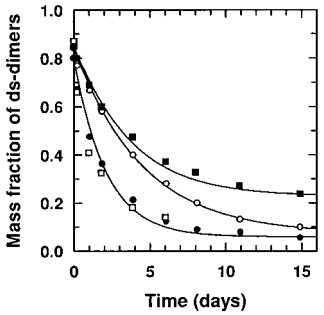

FIGURE 2: Time course dependence of the conformational transition of gA incorporated into SUV vesicles of DOPC (○); DOPG (●), DOPE (□), and DOPS (■) as determined by HPLC. The lipid/peptide film was hydrated with Tris-HCl 15 mM, NaCl 100 mM, pH 7.5, sonicated, centrifuged, and then incubated at 25 °C. The lines correspond to the fitting of the data to eq 2 (see the Materials and Methods section). The peptide concentration was 40 μM, and the peptide/lipid mole ratio was 1:50.

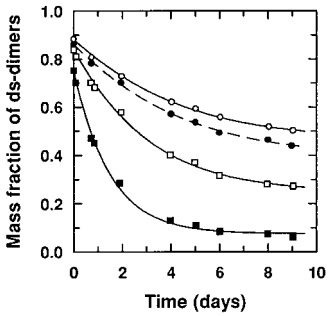

FIGURE 3: Dissociation kinetics at room temperature of gA ds-dimers in SUV vesicles of DOPC (18:1) (○), DPoPC (16:1) (□), DMoPC (14:1) (■), and EPC (●) as determined by HPLC. The lines correspond to the fitting of the data to eq 2 (see the Materials and Methods section). The peptide concentration was 40 μM, and the peptide/lipid mole ratio was 1:50.

conformation of gA, at room temperature, was the monomeric form (not shown) independent of the trehalose concentration present in the samples, although the monomerization rate decreased as the trehalose concentration increased ($k_1 = 2.4 \times 10^{-6}$ s^{-1} in a control sample without sugar, and $k_1 = 1.8 \times 10^{-6}$ s^{-1} and $k_1 = 1.4 \times 10^{-6}$ s^{-1} for trehalose concentrations of 0.5 and 0.75 M, respectively).

The influence of the chemical nature of the lipid polar headgroup on the gA conformational interconversion was analyzed at 25 °C in terms of dissociation kinetics of gA ds-dimers when incorporated in SUV of different pure, zwitterionic and anionic, monounsaturated phospholipids (Figure 2). The monomerization rates changed as a function of the chemical nature of the lipid head, in the order PE $\approx$ PG > PC > PS, although the most stable conformation at long incubations was always the monomeric form. Thus, it seems that the thermodynamically stable conformation is the monomeric state. Furthermore, in parallel experiments, it was verified that after insertion of monomeric gA in each of the phospholipid bilayers, this conformer remained stabilized in the membrane without any further conformational rearrangement. Since the fatty acyl composition was the same for all the phospholipids used, the differences observed can be ascribed to each particular headgroup.

Lipid Acyl Chain Length and Degree of Unsaturation. The effect of short-chain lipids on the stability and conformation of gA has been recently described in spectroscopy experiments using diacylphosphatidylcholines of varying acyl chain length (26). It has been demonstrated that the channel conformation of gA can only be achieved if the number of carbon atoms is higher than 8. Furthermore, CD and Fourier transform infrared studies indicated that gA retains the β-helical structure in PC with saturated acyl chains and with one double bond, whereas in dilinoleoyl-PC (two double bonds in each chain) and soybean-PC (a mixture of molecular species with a high content of the diunsaturated ones) the thermodynamically preferred conformation seems to be double-stranded helices (*28*, *29*).

To quantitatively determine the effect of the acyl chain length on the dissociation of double-helical dimers, gA-containing vesicles were prepared using diacylphosphatidylcholines with two identical monounsaturated acyl chains of varying length. Figure 3 depicts the evolution of the mass fraction of ds-dimers as a function of time in DOPC (di-C18:1), DPoPC (di-C16:1), and DMoPC (di-C14:1) vesicles at 20 °C, the temperature above the gel to liquid/crystalline phase transition for each lipid. A sample of gA in EPC vesicles, in which the dioleoyl C18:1 chain predominates, has been included for comparison. The ds-dimer-to-monomer conformational transition rates increased as the acyl chain length decreased, and at long incubation times, we found that the monomer population is higher for the shorter acyl chain phospholipids than for the longer ones. As an example, at 20 °C the transition rate for DOPC (di-C18:1) was slow enough that after 10 days of incubation more than 50% of ds-dimers still remained. However, when gA was inserted as monomers in bilayers of DOPC, the mass fraction of ds-dimers was below 0.05 in the same time interval. Similar results were obtained when gA was incorporated as monomers in bilayers of soybean-phosphatidylcholine and dilinoleoyl-phosphatidylcholine (di-C18:2) at 23, 45, or 68 °C, and after reasonably long incubation times (not shown). The results reveal that the ds-dimeric conformation could remain as a metastable state in bilayers of long acyl chain length unsaturated lipids that fully agree with previous channel conductance studies (*29*). Furthermore, the thermodynamically stable conformer seems to be monomeric regardless of the phospholipid used in the bilayer preparation.

Presence of Sterols. It is known that sterol molecules can modify the physical properties of synthetic and natural bilayers. We questioned how sterol-induced changes could affect the gA ds-dimer dissociation in the bilayer. The time-dependent dissociation of gA ds-dimers in sterol/EPC vesicles (1:17:50 gA/sterol/EPC ratio), for cholesterol, sitosterol, ergosterol, and 7-dehydrocholesterol is shown in Figure 4A. In all cases the rate of conformational transition from the intertwined ds-dimer-to-monomer conformation was found to be less in sterol-containing vesicles than in sterol-free vesicles. Moreover, the transition rates were dependent on the chemical nature of the sterol molecule (Figure 4A). Furthermore, the conformational transition rates were also dependent on the sterol/EPC mole ratio (Figure 4B). Thus, the transition rate was decreased as the sterol/EPC mole ratio increased. A similar behavior was observed for all the sterols tested in the range 1:5−1:1 sterol/EPC ratios (not shown). For a 1:1 cholesterol/EPC ratio the gA monomerization was not quantitatively significant.

(II) Sequence Modulation of the Conformational and Functional Behavior of Gramicidin A. Prior studies utilizing

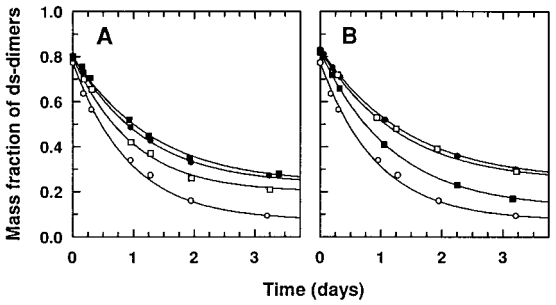

FIGURE 4: HPLC kinetic profiles of the dissociation of gA ds-dimers in EPC SUV at room temperature as a function of the following compounds in panels A and B. (A) The sterol chemical nature, cholesterol (●); sitosterol (□); ergosterol (■); the sterol/EPC mole ratio was 1:3. The kinetic profile for 7-dehydrocholesterol was coincident with ergosterol (■). (B) Sterol (7-dehydrocholesterol)/EPC mole ratio: 1:2 (●), 1:3 (□), and 1:5 (■). (A and B) gA/EPC control sample (○). The lines correspond to the fitting of the data to eq 2 (see the Materials and Methods section). The peptide concentration was 40 μM, and the peptide/EPC mole ratio was 1:50. To verify that the most stable conformational species of gA was the monomeric form independent of the sterol nature and sterol/lipid mole ratio, control samples were prepared containing mainly gA monomers. The mass fraction of ds-dimers at equilibrium was lower than 0.05 in all cases.

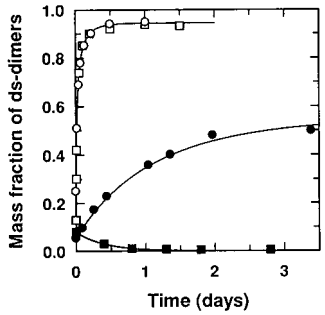

FIGURE 5: Time course of the conformational transitions of W(9,11,13,15)FgA (gM) (○), W(9,11,13,15)NapgA (gN) (□), *N*-formyl gramicidin A (●), and gA (■) in DOPC vesicles, as determined by HPLC. The vesicles were prepared by cosolubilization of the peptide and lipid in TFE and incubated at 50 °C. The lines correspond to the fitting of the data to eq 3, except for gA which were fitted to eq 2 (see the Materials and Methods section). The peptide concentration was 40 μM, and the peptide/lipid mole ratio was 1:50.

Trp → Phe gA substitution analogues have shown that these changes at the peptide's primary sequence exert a complex influence on the channel properties of gA (*49*, *50*). In particular, the gA Trp residues located at the C-terminal end are essential for channel activity (*50*) and for the stabilization of the β-helical conformation (*8*, *9*, *17*, *33*). The HPLC approach offers the possibility to quantitatively analyze how defined side chain modifications or substitutions in the gA primary sequence can modulate the conformational behavior of the peptide in a membrane environment. We have examined the influence of Trp chemical modifications as well as Trp → Phe substitutions on the ds-dimer-to-monomer conformational transition of gA. In all these experiments the samples were prepared by cosolubilization of peptide and lipid in TFE in order to achieve fresh vesicles containing mainly gramicidin monomers (*8*, *23*).

Influence of Chemical Modification or Substitution of All Four Trp Residues on Gramicidin Conformational Preference. Figure 5 shows that in DOPC vesicles gramicidin A, gramicidin M, and gramicidin N have noticeable differences in their conformational behavior. The time course of the peptide conformational interconversion was monitored at 50 °C to accelerate the conformational transitions. In contrast to gA (whose thermodynamically stable conformation was the monomeric form), gM and gN underwent a conformational rearrangement from the starting monomers to double-stranded dimers (mass fraction of ds-dimers > 0.95 for both peptides after 24 h). The behavior observed for gM (Figure 5) was identical to that of its enantiomer gM$^-$ (*8*) in the range of temperature between 23 and 68 °C, and the extent of ds-dimer formation was dependent on the peptide-to-lipid mole ratio (not shown). These results suggest that, independent of the peptide's chirality, linear gramicidins lacking hydrogen bond forming aromatic residues are unstable in the channel conformation in the bilayer and refold toward an energetically preferred double-stranded dimeric structure. At this point, it should be noted that the refolding is not fully completed (and perhaps concentration-dependent), because gM channels are observed at low concentrations (*39*). Remarkably, the gM channels are also right-handed and never left-handed (*39*), and so even Trp-less gM retains sequence information to specify a right-handed channel over a left-handed channel (although double-stranded nonconducting conformations are favored at higher concentrations).

The N-formylation of the indole groups of the four Trp showed less differences between this analogue and the original gA, although a substantial stabilization of double-stranded structures is still observed (Figure 5). Thus, at 50 °C and a peptide-to-lipid mole ratio of 1:50, the mass fraction of ds-dimers became stabilized at a value of 0.50 after 2 days. The proportion of ds-dimers was slightly increased when the sample was incubated at 70 °C.

Influence of Systematic Trp → Phe Replacements of One, Two, or Three Residues in Gramicidin Conformational Preference. To assess the specific role of each individual Trp residue in the peptide conformation when incorporated in a lipid environment, mono-, di-, and tri- Trp → Phe substitution analogues of gA were inserted in DOPC bilayers and analyzed by HPLC. Phenylalanine was chose for three reasons: (i) it is an aromatic residue lacking H-bonding ability, (ii) it exists (as gramicidin B) with Phe instead of Trp at position 11 at a level of 5% in the natural mixture of gramicidin, and (iii) the tetrasubstituted Trp → Phe analogue (gM) shows a conversion higher than 95% from monomers to double-stranded dimers in DOPC bilayers, and it would represent an useful reference to quantify the individual effects originated by partial Trp substitutions.

All the samples were prepared by cosolubilization of peptide and lipid in TFE, except for W(9,11)FgA that was prepared from methanol. Samples were incubated at different temperatures and monitored by HPLC. As an example, Figure 6 depicts the time-dependent conformational transition obtained at 45 °C for mono- (Figure 6A), di- (Figure 6B), and trisubstituted analogues (Figure 6C). The results obtained for gA (Figure 6A) and gM (Figure 6C) have been included for comparison. As expected, when gA was incorporated as a monomer (from TFE), this conformation remained unaltered after a long incubation time (Figure 6A), while for gM the monomers assembled into double-stranded conformers to reach a final equilibrium state with a mass fraction of ds-dimers close to 1.0 (Figure 6C). Note that the ds-dimer/monomer ratio at any given time or at equi-

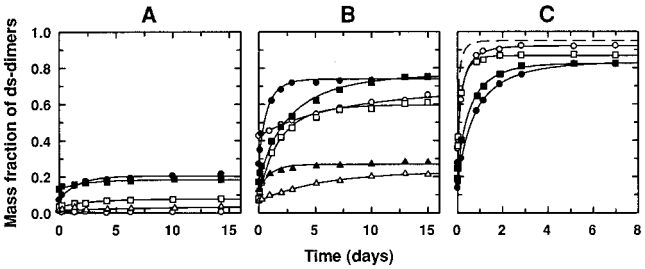

FIGURE 6: Time course of the conformational transition of the Trp → Phe substitution gA analogues in DOPC vesicles at 45 °C, as determined by HPLC. (A): gA (○), W9FgA (●), W11FgA (□), W13FgA (■), and W15FgA (△). (B): W(9,11)FgA (○), W(9,13)FgA (●), W(9,15)gA (□), W(11,13)FgA (■), W(11,15)FgA (△), and W(13,15)FgA (▲). (C): W(9,11,13)FgA (○), W(9,11,15)FgA (●), W(9,13,15)FgA (□), W(11,13,15)FgA (■), and W(9,11,13,15)FgA (gM, dashed curve). All lines correspond to the fitting of the data to eq 3 (see the Materials and Methods section). The peptide concentration was 40 μM, and the peptide/lipid mole ratio was 1:50.

librium depends on the total number of substituted Trp as well as on the substituted position along the peptide sequence (Figure 6). In fact, the monomer refolding into intertwined dimers is facilitated as the total number of Trp substitution increases (mono < di < tri < tetra). As a general behavior for the whole set of substitution analogues, the mass fraction of double-stranded dimers increased upon raising the temperature. Furthermore, at any given temperature, for each mono-, di-, and trisubstituted analogue series, HPLC revealed that positions 9 and 13 are more sensitive, in terms of increased ds-dimer population, to the replacement of Trp by phenylalanine. Therefore, for monosubstituted analogues the mass fraction of ds-dimers at equilibrium was already noticeable for W9FgA and W13FgA (0.2 at 45 °C, Figure 6A) and varied in the order W9FgA ≈ W13FgA > W11FgA > W15FgA. The replacement of two Trp by phenylalanine increased the mass fraction of ds-dimers, especially for analogues W(9,13)FgA and W(9,11)FgA (the equilibrium mass fraction of ds-dimers was 0.70 at 45 °C). However, the mass fraction of ds-dimers for W(11,15)FgA and W(13,15)FgA was only 0.25 at 45 °C (Figure 6B). Comparison of the kinetic profile corresponding to W(11,15)FgA and W(13,15)FgA (Figure 6B) versus W(9,11,15)FgA and W(9,13,15)FgA (Figure 6C) shows that further substitution of Trp → Phe at position 9 increased the double-stranded conformer population. Overall, for trisubstituted analogues the mass fraction of ds-dimers varied between 0.83 (W(9,11,15)FgA) and 0.92 (W(9,11,13)FgA) at this temperature. Similar changes between mono-, di-, and trisubstituted analogues were observed in the mass fraction of ds-dimeric forms after incubation of the samples at 23 and 68 °C (see Table 1 as an example).

Fitting the experimental data from Figure 6 to a monomer/ds-dimer transition (eq 3, Materials and Methods section) indicated that the conformational transition taking place in the lipid membrane can be interpreted in terms of a simple dimerization process for each peptide substitution analogue. These results also validated the accuracy of the chromatographic quantitation in terms of the conformational species of gramicidin analogues in a lipid environment, as previously demonstrated for the natural gramicidin mixture (*23*). Furthermore, analysis of the chromatographic data gave the rate constant, k_{-1}, for the dimerization process for each substitution analogue at three different temperatures (23, 45, and 68 °C). Table 1 summarizes the values of k_{-1} for synthetic gA and for the set of 14 Trp substitution analogues studied here. Table 1 also includes the values corresponding to the equilibrium mass fraction of double-stranded dimers for each peptide analogue at the different temperatures. As the temperature increased, the conformational transition from monomer to double-stranded conformation was accelerated. Also, the higher the number of Trp replacements, the higher the extent and the rate of dimerization. Overall, the data reported here indicate that the contribution of each Trp → Phe substitution along the peptide sequence is different and independent.

Table 1: Mass Fraction of ds-Dimers at Equilibrium and Dimerization Constant (k_{-1}) for Trp → Phe Substitution Gramicidin Analogues in DOPC Vesicles at Different Temperatures[a]

gramicidin	temperature (°C)	$mfdsd_{eq}$	k_{-1} (s^{-1} M^{-1})
gA	23	<0.02	nd
	45	<0.01	nd
	68	0.00	nd
W9FgA	23	0.08	nd
	45	0.21	0.0382
	68	0.32	nd
W11FgA	23	0.04	nd
	45	0.08	0.00801
	68	0.22	nd
W13FgA	23	0.12	nd
	45	0.18	0.0243
	68	0.40	nd
W15FgA	23	0.02	nd
	45	0.04	nd
	68	0.05	nd
W(9,11)FgA	23	0.44	nd
	45	0.67	0.039
	68	0.68	5.60
W(9,13)FgA	23	0.47	nd
	45	0.75	0.441
	68	0.76	32.5
W(9,15)FgA	23	0.15	nd
	45	0.59	0.112
	68	0.70	7.69
W(11,13)FgA	23	0.27	nd
	45	0.75	0.109
	68	0.84	9.64
W(11,15)FgA	23	0.07	nd
	45	0.23	0.012
	68	0.51	1.27
W(13,15)FgA	23	0.12	nd
	45	0.27	0.078
	68	0.51	5.53
W(9,11,13)FgA	23	0.75	0.042
	45	0.92	2.28
	68	0.94	77.5
W(9,11,15)FgA	23	0.45	0.010
	45	0.83	0.41
	68	0.85	18.1
W(9,13,15)FgA	23	0.82	0.070
	45	0.87	2.54
	68	0.87	71.2
W(11,13,15)FgA	23	0.56	0.023
	45	0.83	0.61
	68	0.87	24.5

[a] Peptide concentration, 40 μM; peptide/lipid mole ratio, 1:50; $mfdsd_{eq}$, mass fraction of ds-dimers at equilibrium; nd, not determined.

CD Spectroscopy. The channel conformation ($\beta^{6.3}$-helical structure) of gA is characterized by a unique CD spectrum with a maximum at 220 nm, a minimum at 230 nm, a positive peak at 235 nm, and negative ellipticity below 205 nm (*51*, *52*). It has been previously shown that the channel confor-

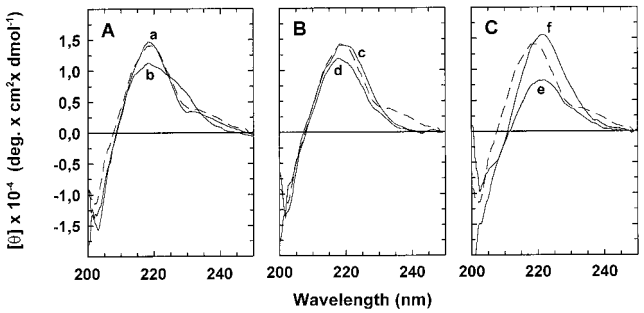

FIGURE 7: Far-ultraviolet CD spectra of the Trp → Phe substitution gA analogues incorporated from TFE in DOPC vesicles: (a) W11FgA; (b) W15FgA; (c) W(9,13)FgA; (d) W(11,15)FgA; (e) W(11,13,15)FgA; and (f) W(9,11,13,15)FgA (gM). The dashed line corresponds to gA. The peptide/lipid mole ratio was 1:50. The peptide concentration was always 40 μM, although in the case of W(9,11,13,15)FgA the actual peptide concentration could be uncertain due to the difficulty of UV concentration determination in the presence of lipid vesicles.

mation can be directly observed when gA is incorporated in model membranes from polar organic solvents such as TFE (*19*, *20*, *24*). Furthermore, the use of HPLC and CD in combination have demonstrated that a nonchannel CD spectrum can be attributed mainly to the contribution of two conformational species, double-stranded dimers and $\beta^{6.3}$-helical monomers, coexisting in the lipid environment in a proportion that is determined by the specific sample preparation protocol (*23*, *24*).

To determine the secondary structure adopted by the Trp substitution analogues in DOPC vesicles, samples for CD spectroscopy were prepared by cosolubilization of peptide and lipid in TFE at 1:50 peptide/lipid ratio, at 4 °C, to achieve fresh samples containing mainly the monomeric form of the peptides. However, as we have shown before, most of the Trp substitution analogues have a high tendency to dimerize, and the dimerization process could have even begun during sample preparation. For this reason, it was not possible to obtain fresh samples containing less than 5% of double-stranded conformers (see the values of mass fraction of ds-dimers at 0 time in Figure 6). Only fresh samples corresponding to gA, W11FgA, and W15FgA analogues contained less than 3% of ds-dimers as deduced from HPLC. It should be noted that the known strategy used to achieve the channel conformation of gA in an overnight sample incubation at high temperature (68−70 °C) was not applicable here because any temperature increment favored the appearance of double-stranded conformers for the whole set of Trp substitution analogues (Table 1). The tendency toward double-stranded conformers upon heating has also been noted previously for gA itself in short lipids (*26*).

As an example, Figure 7 shows the CD spectra for mono- (W11FgA and W15FgA), di- (W(9,13)FgA and W(11,15)-FgA), tri- (W(11,13,15)FgA), and tetra- (W(9,11,13,15)FgA) substitution analogues. The CD spectrum of gA (dashed lines) has been also included for comparison. All of the Trp substitution analogues showed a CD spectrum with a maximum around 220 nm and positive ellipticity at 230 nm. The maximum at 235 nm was only detected for W11FgA, whose spectrum was identical to that of gA, exhibiting the characteristic pattern of the $\beta^{6.3}$-helical configuration. In general, as the number of substituted Trp's increased, we observed a reduced amplitude and a shift of the maximum at 220 nm to higher wavelength, with significant differences depending on the position of substitution of the Trp residue. For W(9,11,13,15)FgA the amplitude was the same relative to gA but a more pronounced shift toward higher wavelength was obtained. The spectrum for W15FgA was similar to that observed for W15AgA analogue in SDS micelles (*53*). The spectra for all Trp substitution analogues paralleled the spectrum of the gA channel form but are not strictly identical. The differences might be explained by the contribution of the aromatic residues to the CD signal in the far-UV region and by the presence, to some extent, of a proportion of double-stranded dimers.

Table 2: Maximum Fluorescence Emission of Gramicidin Trp Substitution Analogues in DOPC Vesicles (λ_{ex} = 280 nm)

gramicidin	monomer emission wavelength[a]	ds-dimer emission wavelength[b]
W(11,13,15)FgA	333	318
W(9,13,15)FgA	335	334
W(9,11,15)FgA	336	336
W(9,11,13)FgA	342	345

[a] Fresh samples prepared from TFE. [b] Samples incubated for 4 h at 68 °C.

Trp Fluorescence. The fluorescence emission properties of an indol group are sensitive to changes in the solvent polarity, and consequently, fluorescence spectroscopy has been extensively used to determine the environment polarity of Trp residues in proteins and peptides, including gA (*54*−*56*). For native gA, the interpretation of the fluorescence spectrum is not obvious due to the presence of four Trp residues in the peptide sequence (eight in the ds-dimer). Spectral measurements are an average response of all fluorophores in the molecule (*34*). Additional difficulties are encountered if a mixture of conformers exists in the sample. Nevertheless, it has been possible to follow non-channel-to-channel conversion on the basis of differences in the fluorescence emission, in lipid bilayers (*55*), and in inverted micelles (*56*). Thus, slight shifts toward lower wavelengths (around 5 nm) were observed as the ds-dimer dissociated (*56*). However, information about the environmental changes undergone by each individual Trp residue, as a consequence of the peptide conformational rearrangement in the membrane, could not be obtained from steady-state fluorescence studies.

Taking advantage of the presence of only one Trp residue in the analogues with three Trp → Phe substitutions, the fluorescence emission spectra can provide an estimation of the environment polarity of each individual Trp residue of gramicidin in the β-helical monomeric structure and in the double-stranded conformation in lipid bilayers. Table 2 shows the fluorescence maxima emission of the four trisubstituted analogues in the monomeric form in DOPC vesicles (mass fraction of ds-dimers was <0.10 as deduced from HPLC). Trp-15 (W(9,11,13)FgA) is located in a rather polar microenvironment but it is not totally water exposed because a full water exposed Trp shows emission maxima at 355 nm (*57*). Trp-13 (W(9,11,15)FgA) is somewhat less water exposed (6 nm blue-shifted relative to Trp-15), whereas Trp-11 (W(9,13,15)FgA) and Trp-9 (W(11,13,15)FgA) are in a hydrophobic microenvironment suggesting that these residues are more deeply buried in the lipid bilayer. The vesicles containing the peptide monomeric forms were later heated

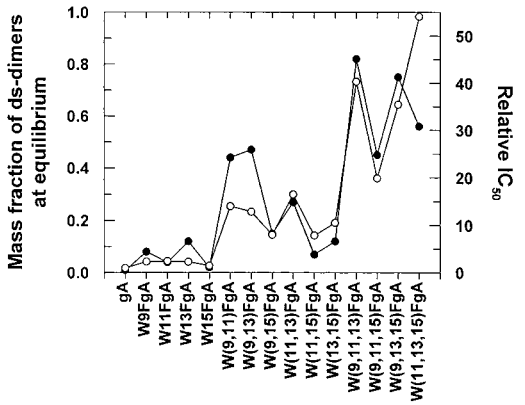

FIGURE 8: (●) Mass fraction of ds-dimers at equilibrium for the Trp → Phe substitution gA analogues in DOPC vesicles at 23 °C, as determined by HPLC. The peptide concentration was 40 μM, and the peptide/lipid mole ratio was 1:50. (○) Relative antibiotic activity against *E. faecium* for Trp → Phe substitution gA analogues, expressed as the peptide concentration inhibiting the bacterial growth to 50% (IC_{50}).

for 4 h at 68 °C in order to induce the dimerization of the peptides (mass fraction of ds-dimers was 0.90). The emission maximum of Trp-9 was blue-shifted 15 nm suggestive of a much less polar environment in the ds-dimeric structure. Trp-15 shifted only three nanometers toward the red (indicative of a slightly more polar medium). The conformational transition induced a slight blue shift (1 nm) for Trp-11 and did not appreciably change the fluorescence spectrum of Trp-13.

The indol excitation spectrum is also sensitive to environment polarity, and it shows, besides the main peak near 280 nm, a sharp peak around 290 nm in apolar media, which becomes a shoulder in water (*58*). Thus, we could corroborate the fluorescence emission results by fluorescence excitation (results not shown).

Antibiotic Assay. We investigated the effect of the Trp → Phe replacements on the antibiotic activity against *E. faecium*. The antimicrobial activity of each substitution analogue was measured using different concentrations to obtain the peptide concentration necessary to inhibit 50% of bacterial growth (IC_{50}, Figure 8). In general, Trp substitutions lowered the antibiotic activity. The replacement of Trp-15 had the smallest effect on the antibiotic activity of the peptide relative to gA, and some differences between peptides with the same number of replacements could be seen. The antibiotic activity correllated with the mass fraction of double-stranded dimeric forms for all Trp substitution analogues (Figure 8).

DISCUSSION

Although is well-known that gA ds-dimers (nonchannel conformation) in lipid bilayers are unstable and refold into the channel conformation, only a limited amount of information currently exists in the scientific literature on the microenvironment parameters involved in that process. In this article we have addressed the following questions: what is the importance of the phospholipid environment in the unwinding of double-stranded structures of gA?; why is the gA channel conformation stabilized in lipid bilayers? and; if hydrogen bonding between Trp and the membrane interface is a driving force for the dissociation of gA ds-dimers, do all Trp have the same importance in this process?

Evidence from previous work in several laboratories, including our own group, suggested that both the physical and chemical nature of the phospholipid membrane and the Trp residues on the gA sequence could have significant contributions to the processes underlying such a conformational transition (*8*, *9*, *15*, *17*, *26*, *27*, *55*). Each of these parameters has been quantitatively investigated in the present paper. We begin the discussion of our results by an examination of the Trp fluorescence of gA analogues having a single Trp residue.

In the antiparallel double helix of the native gA ds-dimer, the eight Trp chains are mostly in a hydrophobic environment uniformly distributed along the helix axis (*25*, *59*). The estimation of the microenvironment of each single Trp in the ds-dimeric conformation has been performed using Trp-trisubstituted gramicidin analogues (Table 2). The fluorescence emission maxima suggested a polar microenvironment for Trp-15, probably water accessible, and a relatively low polarity microenvironment for Trp-11 and Trp-13. The microenvironment for Trp-9 is extremely hydrophobic. For this analogue, the fluorescence emission maximum wavelength (318 nm) suggests that, in the ds-dimer, Trp-9 is forced to be buried close to the center of the bilayer. Due to its amphipathic nature the indol group has the propensity to be localized in interfacial environments (*1*). Thus, this Trp residue is placed in an hostile microenvironment that could be, among others, one of the factors that determines the observed unstability of gA ds-dimers in the lipid medium. It has also been suggested that hydrogen bond formation between Trp residues and the bilayer surface (including the carbonyl group of the phospholipid polar heads) could be a driving force for the unwinding of ds-dimers in the membrane (*17*, *22*, *33*, *34*). As deduced from our results (Figure 1), the hydrogen bonding between the carbonyl group of the phospholipid polar headgroup and the peptide's Trp residues seems not to be a key interaction for the unwinding of ds-dimers, since the rate of ds-dimer dissociation was similar before and after replacement of the ester function by an ether moiety (i.e., without the carbonyl group). Thus, in agreement with Providence et al. (*39*), the interaction between Trp side chains and the ester C═O groups is not important for the unwinding of ds-dimers, nor for channel function. However, we cannot exclude other possibilities of hydrogen bonding between Trp residues and some other polar groups in the membrane interface (*17*, *60*) because we found a significant decrease in the dissociation rate in the presence of trehalose, a sugar with dehydrating effects on the lipid polar head (*46*).

Next, when the degree of unsaturation of the acyl lipid chain was tested, the single-stranded conformation of gA was found to be thermodynamically preferred in bilayers composed of unsaturated lipids (see Figure 3 as an example). The chromatographic results are in concordance with previous fluorescence, CD, and FTIR studies on the nonchannel-to-channel transition of gA in unsaturated phospholipid bilayers (*28*, *55*). Variations of the membrane thickness, by the use of monounsaturated lipids with different acyl chain lengths, resulted in changes in the transition rate from ds-dimers to monomeric forms. In fact, the transition rate decreased as the lipid chain length increased, in line with previously reported results that analyzed, by means of CD spectroscopy, the secondary structure of gA when incorporated in lipid bilayers made of phospholipids with acyl chains

having from 12 to 22 C-atoms in length (*20*). Also, from gA channel experiments, it was observed that lipid bilayer thickness might affect the conformational preference of gA channels favoring the existence of ds-dimers as the bilayer thickness increased (*61*). HPLC experiments with dilinoleoyl-phosphatidylcholine and natural soybean-phosphatidylcholine membranes in which gA was incorporated as monomers indicated that this structure remains stable even after 8 h of incubation at 68 °C. This result contrasts with the previously reported results obtained from CD and FTIR spectroscopy, where parallel and antiparallel double-stranded dimers were identified as the predominant conformational states of gA in these two lipid membranes (*28*). At the present time, the reason for this discrepancy is not clear, but when we reproduced this experiment in our laboratory, we observed a phase separation in samples where gA was incorporated in diunsaturated lipid membranes, associated with a decrease in the monomer peak area. Moreover, we found that the remaining supernatant was clearly enriched in ds-dimers. Furthermore, the reported FTIR spectra of gA in soybean-PC were made using ethanol as an organic solvent in the preparation protocol (*28*). Double-stranded dimers could be present in a significant proportion, in lipid bilayers prepared from ethanol (*21*, *23*), especially at the peptide concentrations used in FTIR experiments (4−5 mM). Recent channel conductance studies with palmitoyl-oleoyl-phosphatidylcholine (POPC), DOPC, and dilinoleoyl-phosphatidylcholine (*n*-decane containing) bilayers did not observe long-lived channels that could be related to conducting double-stranded helical dimers in any of these membrane environments (*29*).

The nature of the lipid head modulates the dissociation rate of ds-dimers in membranes. The importance of this factor is shown by the differences observed in the dissociation rate in experiments where the fatty acyl composition was identical for all the phospholipids, but each one had a different polar headgroup. Interestingly, the increased rate of unwinding of ds-dimeric structures in DOPE relative to DOPC (Figure 2) supports previous fluorescence emission studies that indicated that gA in POPC/POPE bilayers was more rapidly converted into the channel conformation than pure POPC bilayers were (*55*). Moreover, from the analysis of the dimerization kinetics of gA in DOPS at different pH values, a noticeable increase in the dissociation rate was observed as the pH increased (Salom, D., unpublished results). This could be related to the increased membrane fluidity as a result of the presence of two negative charges in the phospholipid polar headgroup.

A decrease in the rate of ds-dimer dissociation could also be expected when sterols are present in the phospholipid vesicles due to a lowered accessibility of the polar heads to the peptide's Trp residues, since in a lipid bilayer gA and cholesterol might interact with each other (*62*−*64*). The formation of a complex between cholesterol and gA has been suggested to explain the decreased channel conductance observed when a 1:5 gA/cholesterol stoichiometry was tested in conductance experiments (*64*). Moreover, the incorporation of sterols into a lipid bilayer in the fluid phase increased the lipid chain order (*65*), bilayer thickness (*66*), and bilayer stiffness (*67*) to a different extent depending on the sterol's chemical structure (*65*). These effects could account for the differences observed in the dissociation rate. In fact, such differences were revealed for all the assayed sterols (Figure 4, A and B). The dissociation rate decreased in the order sitosterol > cholesterol > ergosterol > 7-dehydrocholesterol, although the thermodynamically stable gA conformation in the membrane was always the monomer. It is interesting to note that the dissociation rate was strongly dependent on the sterol/lipid mole ratio: the higher the membrane's sterol content, the slower the unwind of ds-dimers. This could agree with the reported time-dependent gA channel inactivation in cholesterol-containing membranes (*68*), where the rate of channel inactivation was also dependent on the phospholipid-to-cholesterol mole ratio (*64*).

Overall, these results indicate that the membrane's lipid composition is a modulating factor for the rearrangement of gramicidin from double-stranded dimers to β-helical monomers. However, our results suggest that the minimum-energy conformation of gA is always the β-helical monomeric structure (channel state) independent of changes in membrane composition.

As mentioned above, the preference for a β-helical conformation of gA in the lipid milieu might be dictated by a defined orientation of the Trp residues toward the membrane interface. The interfacial region in membranes is characterized by unique motional and dielectric properties distinct from both the bulk aqueous phase and the hydrocarbon-like interior of the membrane (*69*, *70*). The amphipathic character of Trp may explain its interfacial location in membranes due to its hydrogen-bonding capability and favorable electrostatic interactions (*71*). Thus, it is not surprising that for gramicidin M and gramicidin N in which the four Trp's are replaced by the aromatic rings (lacking hydrogen-bonding capabilities), phenylalanine and naphthylalanine, respectively, we found that the preferred conformation was the double-stranded dimeric structure instead of the monomeric one (Figure 5). This result agrees with solid-state NMR studies that have recently identified the double-helical fold of gM as an antiparallel, left-handed, double-stranded conformation (*9*). A double-stranded dimer is also the dominant conformation for the enantiomeric gM^- (*8*). Therefore, it seems clear that without the four indoles (i.e., gN, gM, and gM^-) the double-stranded dimer is the minimum-energy conformational state of gA in the bilayer. These results reinforce previous suggestions that Trp residues in gramicidin provide the driving force needed for the stabilization of the single-stranded channel structure (*17*, *22*, *33*). An additional experimental contribution to highlight Trp as key residues is provided from experiments using N-formylated gramicidin where the Trp N−H group is chemically modified to N−CHO, and a mixture of both ds-dimeric and monomeric conformations is present at equilibrium (Figure 5). Our results agree with those from other groups that showed that N-formylated gA induced an important decrease in the induction of the H_{II} phase (*72*), lipid flip-flop (*73*), and membrane fusion relative to native gA (*74*), that would be related with its relatively high propensity to adopt ds-dimeric structures.

The specific role of each Trp residue was investigated here by peptide substitution analogues. We have used a set of 14 gA analogues with systematic Trp → Phe substitutions. Our results indicate that, except for the analogue W15FgA, Trp → Phe substitutions destabilize the monomeric structure in the order tetra- > tri- > di- > monosubstituted analogue,

and that the effect of each substitution is different but nearly independent (Figure 6 and Table 1). Moreover, it is not only the substitution but also the position of the residue that is crucial to determine the stability of the monomeric forms. Thus, for monosubstituted analogues, the mass fraction of monomers is identical for W15FgA relative to gA, whereas double-stranded dimeric species seem to be somewhat stabilized for W9FgA, W13FgA, and W11FgA. Interestingly, recent NMR studies on the effects of the sequential replacement of one single Trp by glycine on the heterogeneity of gramicidin species in SDS micelles showed that there was no detectable effect at position 15 (substitution analogue W15GgA), and that W9GgA showed at least two different conformations at a 1:307 peptide/SDS ratio (*53*). Moreover, temperature increments did not seem to force the system into a single species in SDS micelles as we observed for W9FgA in DOPC bilayers where a mixture of ds-dimers and monomers exists (Table 1). Replacement of Trp-11 by Phe induced the formation of ds-dimers, but the effect was less noticeable than for position 9 (0.22 mass fraction versus 0.32 at 68 °C) in accordance with the reported heterogeneity changes shown for the W11GgA analogue compared to W9GgA (*53*). The presence of ds-dimers in W11FgA analogue (gramicidin B in the natural mixture) is also in agreement with previous results reported by Sawyer et al. (*75*) since gramicidin B was unable to exhibit the characteristic channel CD pattern. On the basis of the parallelism observed between Phe and Gly substitution analogues, it seems that the conformational heterogeneity described in SDS micelles could be ascribed to the existence of a mixture of double-stranded dimeric and monomeric structures. The relative abundance of each structure will be defined by the nature of the model membrane and preparation protocol. Also, it is reasonable to expect that the ds-dimer/monomer ratio can be influenced by the position where the substitution is made. That could account for the differences observed for W9AgA and W15AgA relative to W9GgA and W15GgA analogues (*53*).

The increase in the mass fraction of ds-dimers was much more significant for di- and tri-Trp substitution analogues. The degree of the effect depended on the position of the substitution, especially for di-substituted analogues where the values at equilibrium are between 0.23 (W(11,15)FgA) and 0.75 (W(9,13)FgA) at 45 °C (Table 1). At this temperature, the double-stranded conformation predominates for W(9,13)FgA, W(11,13)FgA, W(9,11)FgA, and W(9,15)-FgA, and for all analogues in the trisubstituted series. These results are in agreement with recent observations on hybrid gA/gM structures which adopt a left-handed double helical structure with at least two buried indole groups (*9*). Furthermore, in both di- and trisubstituted series the importance of each residue in the adoption of ds-dimeric structures follows the same order that was deduced from monosubstituted analogues, Trp-9 $\approx$ Trp-13 > Trp-11 > Trp 15 (Figure 6). Overall, with a single exception (W15FgA), the chromatographic results indicate that the mass fraction of double-stranded forms increases as the number of indol groups in the peptide sequence decreases. This general trend reinforces previous suggestions that nearly a full contingent of indoles is necessary to induce the structural interconversion toward the single-stranded conformation (*9*). In fact, Trp-13, Trp-11, and Trp-9 are needed to induce a quantitative conversion from double-stranded dimers to helical monomers.

Variations in the interconversion rates from ds-dimer to monomer of Trp → Phe substitution analogues of gA have provided new information on the role of each residue. It should be noted that the four Trp in gA are located in the C-terminal moiety, and from experiments of water accessibility using Raman spectroscopy (*31*, *37*), and from our own fluorescence spectroscopy results (Table 2), a consensus microenvironment could be defined for each single Trp residue in the gA monomer. Thus, Trp-15 is in a rather polar microenvironment so it could be accessible to water molecules, Trp-9 is buried in the bilayer and hardly accessible to water (*31*, *37*), and Trp-11 and Trp-13 are less buried in comparison with Trp-9 and its water accessibility depends on the membrane thickness (*31*). Since the Trp environments seem to be clearly defined and the contribution of each residue to the monomer stabilization has been quantitatively described in this work, we can try to correlate this new information with previous reported data about the importance of hydrogen bonding in the stabilization of the monomeric $\beta^{6.3}$-helical conformation of gA. Theoretical (*35*, *36*) and experimental (*25*) studies indicated the presence of hydrogen bond formation between Trp residues and the lipid carbonyl ester groups. More specifically, a strong H-bond between gA Trp-15 and the lipid carbonyl group has been suggested for the peptide in DPPC membranes (*76*). Moreover, when the lipid ester linkage is replaced by an ether linkage the H-bond formed is weaker, and structural and functional consequences were observed, such as a reduced contraction of the channel entrance and a decrease in the peptide-mediated Na^+ transport rate (*76*). In contrast, Providence et al. (*39*) have reported that the ester C═O groups in diacylphospholipids do not interact with the indole NH moieties in gramicidin channels. In light of our chromatographic results, it seems that, in fact, hydrogen bonding between Trp-15 and the lipid carbonyl groups is not essential for the stabilization of the channel state since the analogue W15FgA remained as a monomer in the bilayer. Moreover, we could also postulate that Trp-9 and Trp-13 would have a global higher propensity to hydrogen bond than Trp-11. In fact, our results suggest a stabilization of ds-dimers versus monomers after substitution of Trp-9 or Trp-13. The effect was more pronounced when both substitutions were present, for example, W(9,13)FgA, W(9,11,13)FgA, and W(9,13,15)-FgA. In other words, it seems that the more essential Trp residues for the stabilization of the monomeric conformation are Trp-9 and Trp-13.

Since gA possesses antimicrobial properties against Gram positive bacteria, the Trp substitution analogues used in this study were examined for their effects on *E. faecium*. Overall, Trp → Phe substitution in gramicidin greatly decreased its antibiotic activity (Figure 8). As mentioned above, the monomer conformation of gramicidin (potential channel state) is unstable when the Trp residues are replaced by Phe. This effect is temperature-dependent and more pronounced as the number of Trp → Phe substitutions increases. Although in the biological assays all the peptide analogues were added from DMSO (>95% of monomers from HPLC), a partial rearrangement to ds-dimeric structures could take place during bacterial growth at 37 °C. Our results suggest that as the proportion of ds-dimers increases, the antibiotic activity decreases (higher IC_{50} values, Figure 8). If one

supposes that the monomers are the biologically active species, lower activity would be expected as the number of replacements increases since less monomers are available to form conducting states. This seems to be the case although other explanations cannot be ruled out. For example, it has been shown that Trp → Phe gramicidins form channels equivalent to that of gA, but the channel-forming potency and the conductance decrease as the number of Trp → Phe substitutions increases (*49*). A complete Trp → Phe substitution causes a 20-fold decrease in single-channel conductance and lowers the average single-channel duration (*77*). Moreover, the peptide concentration needed to obtain the same channel appearance rate does increase for analogues in which all four Trp's are replaced by aromatic residues such as naphthylalanine (*50*). It is worth noting that CD spectra for all of the Trp → Phe substituted gramicidins in their monomeric forms were similar to that observed for monomeric gA (Figure 7). Therefore, all of the analogues seem to be able to adopt the typical single-stranded, right-handed $\beta^{6.3}$-helix (channel conformation). This is consistent with planar bilayer experiments which indicate that channels formed from Trp → Phe substituted gramicidins have a single, predominat β-helical backbone conformation that is equivalent to that of gA (*49*).

In conclusion, in the present work we have shown that in membranes, independent of the lipid chemical composition, the ds-dimer conformation of gA is unstable. Variations in the monomerization rates of gA ds-dimers in different lipid environments have provided new information on the role of peptide/lipid interactions in the dissociation process. Thus, membrane composition maintains the gA double-stranded conformation kinetically trapped in the bilayer. Studies of Trp → Phe substitution analogues have allowed us to dissect the importance of each Trp residue in the gramicidin sequence for the stabilization of the monomeric (channel) conformation of the peptide. The analysis of the parameters that influence the ds-dimer/monomer interconversion (concerning both the host bilayer and the peptide sequence) provides additional insights on the molecular basis for gramicidin channel stabilization in membranes.

ACKNOWLEDGMENT

We thank James D. Lear for critical reading of the manuscript.

REFERENCES

1. Jacobs, R. E., and White, S. H. (1989) *Biochemistry 28*, 3421−3437.
2. Popot, J.-L., and Engelman, D. M. (1990) *Biochemistry 29*, 4032−4037.
3. DeGrado, W. F., and Lear, J. D. (1985) *J. Am. Chem. Soc. 107*, 7684−7689.
4. Liu, L. P., Li, S. C., Goto, N. K., and Deber, C. M. (1996) *Biopopymers 39*, 465−470.
5. Blondelle, S. E., Forood, B. F., Houghten, R. A., and Pérez-Payá, E. (1997) *Biopolymers 42*, 489−498.
6. Busath, D. D. (1993) *Annu. Rev. Physiol. 55*, 473−501.
7. Koeppe, R. E., II, and Andersen, O. S. (1996) *Annu. Rev. Biophys. Biomol. Struct. 25*, 231−258.
8. Salom, D., Bañó, M. C., Braco, L., and Abad, C. (1995) *Biochem. Biophys. Res. Commun. 209*, 466−473.
9. Cotten, M., Xu, F., and Cross, T. A. (1997) *Biophys. J. 73*, 614−623.
10. Veatch, W. R., Fossel, E. T., and Blout, E. R. (1974) *Biochemistry 13*, 5249−5256.
11. Veatch, W. R., and Blout, E. R. (1974) *Biochemistry 13*, 5257−5264.
12. Bystrov, V. F., and Arseniev, A. S. (1988) *Tetrahedron 44*, 925−940.
13. Braco, L., Abad, C., Campos, A., and Figueruelo, J. E. (1986) *J. Chromatogr. 353*, 181−192.
14. Bañó, M. C., Braco. L., and Abad, C. (1988) *J. Chromatogr. 458*, 105−116.
15. Abdul-Manan, N., and Hinton, J. F. (1994) *Biochemistry 33*, 6773−6783.
16. Braco, L., Chillaron, F., Bañó, M. C., De la Guardia, M., and Abad, C. (1987) *Spectrochim. Acta 43A*, 1365−1370.
17. Zhang, Z., Pascal, S. M., and Cross, T. A. (1992) *Biochemistry 31*, 8822−8828.
18. Xu, F., Wang, A., Vaughn, J. B., and Cross, T. A. (1996) *J. Am. Chem. Soc. 118*, 9176−9177.
19. LoGrasso, P. V., Moll, F., III, and Cross, T. A. (1988) *Biophys. J. 54*, 259−267.
20. Killian, J. A., Prasard, K. U., Hains, D., and Urry, D. V. (1988) *Biochemistry 27*, 4848−4855.
21. Bañó, M. C., Braco. L., and Abad, C. (1989) *FEBS Lett. 250*, 67−71.
22. O'Connell, A. M., Koeppe, R. E., II, and Andersen, O. S. (1990) *Science 250*, 1256−1259.
23. Bañó, M. C., Braco. L., and Abad, C. (1991) *Biochemistry 30*, 886−894.
24. Bañó, M. C., Braco. L., and Abad, C. (1992) *Biophys. J. 63*, 70−77.
25. Bouchard, M., and Auger, M. (1993) *Biophys. J. 65*, 2484−2492.
26. Greathouse, D. V., Hinton, J. F., Kim, K. S., and Koeppe, R. E., II (1994) *Biochemistry 33*, 4291−4299.
27. Arumugan, S., Pascal, S., North, C. L., Hu, W., Lee, C., Cotten, M., Ketchem, R. R., Xu, F., Brenneman, M., Kovacs, F., Tian, F., Wang, A., Huo, S., and Cross, T. A. (1996) *Proc. Natl. Acad. Sci. U.S.A. 93*, 5872−5876.
28. Sychev, S. V., Barsukov, L. I., and Ivanov, V. T. (1993) *Eur. Biophys. J. 22*, 279−288.
29. Girshman, J., Greathouse, D. V., Koeppe, R. E., II, and Andersen, O. S. (1997) *Biophys. J. 73*, 1310−1319.
30. Urry, D. W. (1971) *Proc. Natl. Acad. Sci. U.S.A. 68*, 672−676.
31. Takeuchi, H., Nemoto, Y., and Harada, I. (1990) *Biochemistry 29*, 1572−1579.
32. Scarlatta, S. F. (1991) *Biochemistry 30*, 9853−9859.
33. Hu, W., Lee, K. C., and Cross, T. A. (1993) *Biochemistry 32*, 7035−7047.
34. Mukherjee, S., and Chattopadhyay, A. (1994) *Biochemistry 33*, 5089−5097.
35. Woolf, T. B., and Roux, B. (1994) *Proc. Natl. Acad. Sci. U.S.A. 91*, 11631−11635.
36. Woolf, T. B., and Roux, B. (1996) *Proteins: Struct., Funct., Genet. 24*, 92−114.
37. Maruyama, T., and Takeuchi, H. (1997) *Biochemistry 36*, 10993−11001.
38. Pascal, S. M., and Cross, T. A. (1993) *J. Biomol. NMR 3*, 495−513.
39. Providence, L. L., Andersen, O. S., Greathouse, D. V., Koeppe, R. E., II, and Bittman, R. (1995) *Biochemistry 34*, 16404−16411.
40. Houghten, R. A. (1985) *Proc. Natl. Acad. Sci. U.S.A. 82*, 5131−5135.
41. Singleton, W. S., Gray, M. S., Brown, M. L., and White, J. C. (1965) *J. Am. Oil Chem. Soc. 42*, 53−56.
42. Salom, D., and Abad, C. (1996) *J. Chromatogr., A 725*, 315−322.
43. Mingarro, I., Abad, C., and Braco, L. (1994) *Biochemistry 33*, 4652−4660.
44. New, R. R. C. (1990) in *Liposomes, a practical approach* (New, R. R. C., Ed.) pp 105−161, IRL Press, Oxford University Press, Oxford, New York, and London.

45. Killian, J. A., Burger, K. N. J., and De Kruijff, B. (1987) *Biochim. Biophys. Acta 897*, 269−284.
46. Hauser, H. (1981) *Biochim. Biophys. Acta 646*, 203−210.
47. Crowe, L. M., and Crowe, J. H. (1991) *Biochim. Biophys. Acta 1064*, 267−274.
48. Viera, L. I., Alonso-Romanowski, S., Borovyagin, V., Feliz, M. R., and Disalvo, E. A. (1993) *Biochim. Biophys. Acta 1145*, 157−167.
49. Becker, M. D., Greathouse, D. V., Koeppe, R. E., II, and Andersen, O. S. (1991) *Biochemistry 30*, 8830−8839.
50. Fonseca, V., Daumas, P., Ranjalahy-Rasoloarijao, L., Heitz, F., Lazaro, R., Trudelle, Y., and Andersen, O. S. (1992) *Biochemistry 31*, 5340−5350.
51. Urry, D. W., Spisni, A., and Khaled, M. A. (1979) *Biochem. Biophys. Res. Commun. 88*, 940−949.
52. Killian, J. A., Nicholson, L. K., and Cross, T. A. (1988) *Biochim. Biophys. Acta 943*, 535−540.
53. Hinton, J. F., Washburn-McCain, A. M., Snow, A., and Douglas, J. (1997) *J. Magn. Reson. 124*, 132−139.
54. Masotti, L., Cavatorta, P., Sartor, G., Casali, E., and Szabo, A. G. (1986) *Biochim. Biophys. Acta 862*, 265−272.
55. Cox, K. J., Ho, C., Lombardi, J. V., and Stubbs, C. D. (1992) *Biochemistry 31*, 1112−1118.
56. Salom, D., Abad, C., and Braco, L. (1992) *Biochemistry 31*, 8072−8079.
57. Pérez-Payá, E., Porcar, I., Gómez, C. M., Pedrós, J., Campos, A., and Abad, C. (1997) *Biopolymers 42*, 169−181.
58. Lakowicz, J. R. (1983) in *Principles of Fluorescence Spectroscopy*, pp 342−380, Plenum Press, New York and London.
59. Langs, D. A., Smith, G. D., Courseille, C., Precigoux, G., and Hospital, M. (1991) *Proc. Natl. Acad. Sci. U.S.A. 88*, 5345−5349.
60. Durkin, J. T., Providence, L. L., Koeppe, R. E., II, and Andersen, O. S. (1992) *Biophys, J. 62*, 145−159.
61. Mobashery, N., Nielsen, C., and Andersen, O. S. (1997) *FEBS Lett. 412*, 15−20.
62. Gasset, M., Killian, J. A., Tournois, H., and De Kruijff, B. (1988) *Biochim. Biophys. Acta 939*, 79−88.
63. Lev, A. A. (1990) *Biophys. Membr. Transp. 10*, 231−250.
64. Schagina, J. A., Korchev, Y. E., Grinfeldt, A. E., Lev, A. A., and Blasko, K. (1992) *Biochim. Biophys. Acta 1109*, 91−96.
65. Urbina, J. A., Pekerar, S., Le, H., Patterson, J., Montez, B., and Oldfield, E. (1995) *Biochim. Biophys. Acta 1238*, 163−176.
66. Davis, J. H., Bloom. M., Butler, K. W., and Smith, I. C. P. (1980) *Biochim. Biophys. Acta 597*, 477−491.
67. Lundbaek, J. A., Birn, P., Girshman, J., Hansen, A. J., and Andersen, O. S. (1996) *Biochemistry 35*, 3825−3830.
68. Schagina, L. V., Blasko, K., Grinfeldt, A. E., Korchev, Y. E., and Lev, A. A. (1989) *Biochim. Biophys. Acta 978*, 145−150.
69. Gawrisch, K., Barvy, J. A., Holte, L. L. Sinnwll, T., Bergelson, L. D., and Ferretti, J. A. (1995) *Mol. Membr. Biol. 12*, 83−88.
70. Lewis, R. N. A. H., Pohle, W., and McElhaney, R. N. (1996) *Biophys. J. 70*, 2736−2746.
71. Chattopadhyay, A., Mukherjee, S., Rukmini, R., Rawat, S. S., and Sudha, S. (1997) *Biophys. J. 73*, 839−849.
72. Killian, J. A., Timmermans, J. W., Keur, S., and De Kruijff, B. (1985) *Biochim. Biophys. Acta 820*, 154−156.
73. Classen, J., Haest, C. W. M., Tournois, H., and Deuticke, B. (1987) *Biochemistry 26*, 6604−6612.
74. Tournois, H., Fabrie, C. H. J. P., Burger, K. N. J., Mandersloot, J., Hilgers, P., Van Dalen, H., De Gier, J., and De Kruijff, B. (1990) *Biochemistry 29*, 8297−8307.
75. Sawyer, D. B., Williams, L. P., Whaley, W. L., Koeppe, R. E., II, and Andersen, O. S. (1990) *Biophys. J. 58*, 1207−1212.
76. Meulendijks, G. H. W. M., Sonderkamp, T., Dubois, J. E., Nielen, R. J., Kremers, J. A., and Buck, H. M. (1989) *Biochim. Biophys. Acta 979*, 321−330.
77. Daumas, P., Heitz, F., Ranjalahy-Rasoloarijao, L., and Lazaro, R. (1989) *Biochimie 71*, 77−81.

BI980733K